Fisheries Research 270 (2024) 106895

Contents lists available at ScienceDirect

Fisheries Research

journal homepage: www.elsevier.com/locate/fishres

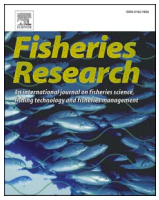

Role of material properties in acoustical target strength: Insights from two species lacking a swimbladder

A. Ladino [a], I. Pérez-Arjona [a,*], V. Espinosa [a], M. Chillarón [a], V. Vidal [a], L.M. Godinho [b], G. Moreno [c], G. Boyra [d]

[a] Universitat Politècnica de València (UPV), Camí de Vera (s/n), 46022 València, Spain
[b] ISISE, Departamento de Engenharia Civil, Universidade de Coimbra, Rua Luís Reis Santos - Pólo II da Universidade, 3030-788 Coimbra, Portugal
[c] International Seafood Sustainability Foundation (ISSF), IEO, 601 New Jersey Ave NW Suite 2020, Washington DC 20001, USA
[d] Azti Foundation, Herrera Kaia, Portualdea z/g, Pasaia 20110, Spain

ARTICLE INFO

Handled by A.E. Punt

Keywords:
Acoustics
Target strength
Backbone
Flesh
Atlantic mackerel
Skipjack tuna

ABSTRACT

Acoustic target strength (TS) is a key parameter for species identification and stock assessment in fisheries. The TS of fish is influenced by the contrast in acoustic impedance between their tissues and the surrounding water. While the swimbladder is responsible for most of the backscatter in fish with gas-filled swim bladders, the backscatter in bladderless fish is a combination of that of fish tissues. The aim of this paper is to explain the marked differences in acoustic properties reported between skipjack tuna and Atlantic mackerel, two important pelagic fish species that lack a swimbladder. The study measures the acoustic properties (density and sound speed) of their flesh and backbone. These measurements are then used to simulate acoustic backscattering using a numerical model based on the Method of Fundamental Solutions, covering a range of frequencies and fish lengths relevant to fisheries acoustics. The numerical estimation of the TS shows that the differences in the material properties of the tissues predict the reported differences in the reduced target strength of more than 10 dB greater for skipjack than for mackerel at 38 kHz and 120 kHz. The study contributes to the understanding of the complex acoustic field backscattered by bladderless fish species and provides insights into the role of fish tissue material properties in the interpretation of acoustic response differences between species.

1. Introduction

Computer simulations of the acoustic backscattering of fish are important because they help to understand the acoustic responses obtained with scientific and commercial echosounders and sonars, which are widely used to detect and study fish populations. Understanding the backscattering can improve the acoustic-based estimates of abundance as well as the discrimination between species and fish sizes.

The acoustic response of fish depends on the contrast between the acoustic impedances of their tissues and organs and the acoustic impedance of the surrounding medium (water). Because the acoustic impedance of fish flesh and bones is closer to that of seawater than that of gases, this accounts for more than 95 % of the backscatter (Foote, 1980) when fish have a gas-filled swimbladder. As the swimbladder typically has a spheroidal shape, acoustic backscattering models of bladder fishes can rely on variations of the model of a spherical air bubble (Andreeva, 1964; Furusawa, 1988; Kloser et al., 2002), which are relatively simple to implement and provide reasonably accurate results (Clay and Home, 1994; González et al., 2013; Macaulay et al., 2013; Prario et al., 2015; Puig-Pons et al., 2022; Spence and Granger, 2005; Tang et al., 2009).

However, in absence of a swimbladder, the responsible for the acoustic backscattering of fish is a combination of the backscattering of their organs (bones, skull, flesh and internal tissues) which have complex morphological structures that are not as easy to simulate as a spheroid, and have provided less successful, and sometimes divergent, modelling results (Forland et al., 2014; Gorska et al., 2005; Nesse et al., 2009). Typical models used to predict acoustic backscattering of bladderless fish species found in bibliography are DWBA (Chu et al., 1993; Stanton and Chu, 2000), KRM (Kloser and Horne, 2003) or FEM (Forland et al., 2014).

Recently, a paper by Boyra et al. (2018) estimated the relationship between in situ target strength (*TS; dB re 1 m^2*) and length (cm) of skipjack tuna (*Katsuwonus pelamis*), a commercially important

* Corresponding author.
E-mail address: iparjona@upvnet.upv.es (I. Pérez-Arjona).

https://doi.org/10.1016/j.fishres.2023.106895
Received 1 June 2023; Received in revised form 23 October 2023; Accepted 23 October 2023
Available online 8 November 2023

bladderless species, typically caught near Fish Aggregating Devices (FADs). The resulting reduced target strength or b_{20} values ($b_{20} = TS - 20\log(L)$, (Simmonds and MacLennan, 2005); measured in dB, commonly used to compare TS values among different species, showed a difference of ~10 dB from those published for Atlantic mackerel (*Scomber scombrus*), a striking difference considering that they are both species without swimbladders. The authors used a FEM (Jech et al., 2015) backscattering simulation to try to explain the obtained differences between species. However, the simulation was short in information about material properties of skipjack tuna's tissues, absent from bibliography. In addition, it could not be run through the full range of acoustic frequencies and fish lengths present in the measurements due to computing constraints (Boyra et al., 2018).

There is a lack of information regarding the material properties of fish tissues and only a few works have addressed the quantification of density and sound speed in fish flesh (Shibata, 1970; Sigfusson et al., 2001; Sigfusson et al., 2001; Yasuma et al., 2009). Previous works reported sound speed measurements referred only to a very limited number of species. To the best of our knowledge, there is absence of works measuring the sound velocity in fish backbone. In the case of bladderless species, differences among material properties, such as densities and sound speeds in flesh and backbones, become more relevant for the backscattered acoustic field than in species with swimbladders. These differences could lead to significant variations in TS values. A better understanding of density and sound speed for different species can facilitate more accurate numerical models and aid in interpreting TS measurements for bladderless species.

In this paper, we aim to elucidate the differences between the acoustic properties of two important bladderless pelagic species, skipjack tuna (SKJ) and Atlantic mackerel (MAC). To this end, we carried out measurements of the acoustic properties (sound speed and density) on flesh and backbone from both species. Using these values, we simulated the acoustic backscattering associated to both species using a numerical model based on the Method of Fundamental Solutions (Pérez-Arjona et al., 2018). The model was solved using the QR decomposition method (Golub and Loan, 2013), which allows to overcome the maximum acoustic frequency and fish length limitations of FEM models, thus increasing the simulated working frequency, covering part of the range of typical frequencies of transducers used in fisheries acoustics, as well as the common range of fish body lengths of both species. The computationally obtained b_{20} parameter for each species was compared and interpreted using previously reported experimental data. Based on these results we attempt to investigate the role of the acoustic properties to interpret and explain some of the differences of the acoustic response between both fish species and, in general, increase our understanding of the complex acoustical field backscattered by bladderless species.

2. Material and methods

To characterize the acoustic impedance (z), calculated as the product of sound speed (c) and volumetric mass density (ρ), it was imperative to determine both c and ρ for the flesh and backbone of the two distinct species: Atlantic mackerel and skipjack tuna. The measurement of each parameter required a different experimental setup.

Skipjack tuna samples were procured from individuals captured during oceanic surveys and immediately frozen. In contrast, the source of Atlantic mackerel samples varied. Some mackerel samples were obtained from frozen individuals, while others were freshly captured, allowing us to conduct measurements on the same day as their capture.

2.1. Measurement of sound speed

The target material was placed between, and in contact with, two 120 kHz Q-low Airmar transducers mounted on sliding holders, the first transducer being used as an ultrasonic source and the second as a receiver (Fig. 1). The emitted signal was generated with a signal function generator Tektronix AFG2021 and a radio-frequency power amplifier (E&I 1040 L, 400 W, amplification up to +55 dB, Rochester, NY). Both the signal excited on the terminals of the first transducer (Emit) and that received through the target material (Rec) were displayed on a digital oscilloscope Tektronix TDS2022C, controlled with a personal computer via the Tektronix software (VISA- *Virtual Instrument Software Architecture*). The Emit and Rec signals were registered to be further analyzed with own code developed on MATLAB®.

The system was calibrated for sound speed in fresh water at room temperature ($T = 25.3 \pm 0.1\,^{o}C$) using a 5-cycles sinusoidal burst with amplitude 10 V peak-to-peak (V_{pp}) at 120 kHz central frequency emitted signal. The measurements were performed varying the distance between transducers, submerged in fresh water, from 1 to 10 cm, with 1 cm intervals. The sound speed, c, was calculated as the slope of the linear relation between t_F and d, being d the distance path between the transducers and t_F the flying time between Emit and Rec signals. We calculated the eigen-correlation of Emit and the cross-correlation between Rec and Emit: the flying time was calculated as the difference

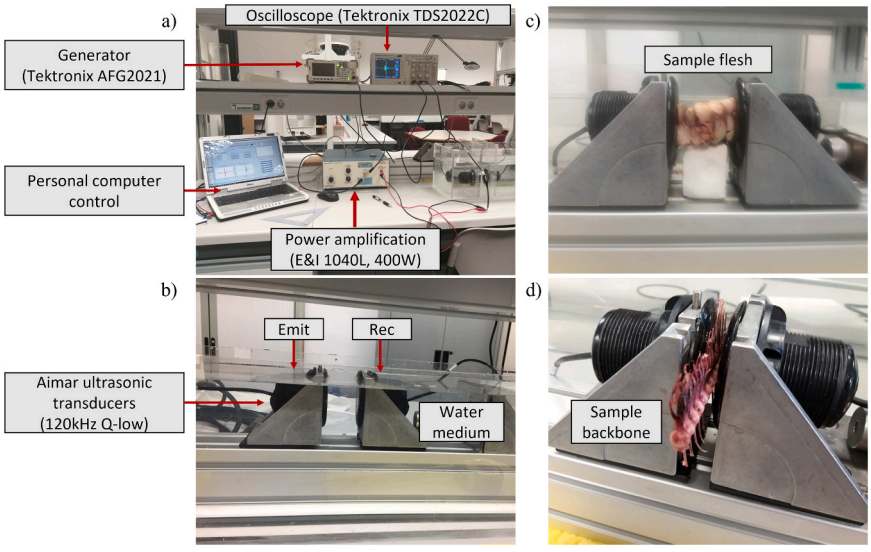

Fig. 1. Experimental setup for the sound speed measurement in tissues. (a) Experimental set-up configuration. (b) System calibration. Example of measurement: Atlantic mackerel sample flesh (c) and (d) Skipjack tuna sample backbone.

between the maxima of eigen and cross-correlation signals. The obtained c value was compared with the prediction from (Lubbers and Graaff, 1998). The intersection with the horizontal axis from the linear regression equation provided the time response (t_R) of the system to be considered in further measurements.

The same procedure was applied to measure the flesh of both Atlantic mackerel and skipjack tuna. The flesh, positioned between and in direct contact with two transducers, was prepared by peeling it and cutting it into slices with widths of 1 cm for Atlantic mackerel and 2 cm for skipjack tuna, each with an area of 4×4 cm^2. To vary the distance between the transducers, additional pieces of flesh were added, and sound speed was determined by establishing a linear relationship between distance and flight time.

To ensure consistent conditions for the flesh and prevent deformations caused by excessive contact pressure, a torque wrench was employed. The torque wrench was set to the minimum torque required to secure the sample (0.1 N m). The excitation signal consisted of a sinusoidal burst with a central frequency of 120 kHz and an amplitude ranging from 10 to 200 V peak-to-peak (V_{pp}) at the transducer terminals. The specific amplitude was adjusted as needed to ensure accurate reception at the end of the samples. The emitted burst consisted of a variable number of cycles (1–5) depending on the length of the samples. Longer pulses were used for longer tissue paths. For precise time-of-flight measurements, the received signal was cross-correlated with the emitted signal, following the same methodology employed in water calibrations.

The evolution of sound speed during the thawing process was monitored at intervals of 5–10 min. The sound speed initially decreased until it reached a plateau, which occurred after approximately 150 min at a room temperature of 24 °C. This plateau displayed a nearly constant sound speed, which, for mackerel, closely matched the value observed in fresh samples and remained stable for over 2 h. Measurements were conducted within this period for both species.

To obtain an estimation of the speed of the compressional acoustic waves in backbone, we used the same emitted signal as for the flesh samples but limiting the number of cycles to 1 cycle, due to the width of the samples. Two samples of backbone, one for Atlantic mackerel and one for skipjack tuna, were selected and located between the transducers. We performed 12 measurements for each species, ensuring good dispersion values, changing the bone orientation and position to obtain an averaged estimation of sound speed. Sound speed was individually calculated as $c = d/(t_F - t_R)$ for each measurement and an averaged value was provided to perform numerical evaluation of TS.

2.2. Measurement of mass density

We measured at first step the density of Atlantic mackerel to compare it with published data (Gorska et al., 2005, 2007) and later we characterized the density of skipjack tissues. Volumetric mass density is defined as:

$$\rho = \frac{m}{V} \tag{1}$$

being m (kg) the mass and V (m^3) the volume of the sample. Mass was directly measured using a *KERN EW600–2 M* balance with a precision of 0.01 g. To measure the sample volume a method based on Archimedes' principle was used. The sample was immersed in distilled water and the weight of the water that the object displaced was measured using the same *KERN EW600–2M* balance that was used for measuring the mass of the sample. Taking into account the density of water, $\rho_w = 10^3 kg/m^3$, once the water weight (m_w) is known, the water volume (V_w) is also determined, $V_w = \rho_w \bullet m_w$, and it is the same as the sample volume $V = V_w$ (Archimedes' principle). This is a common method used in jewelry and medicine (Nordt et al., 1999).

To measure the density of Atlantic mackerel tissues, we employed a single sample of flesh and one sample of backbone. This approach allowed us to make comparisons with previously reported data (Gorska et al., 2005, 2007) and ensure the method's appropriateness. In the case of skipjack tuna, we expanded our measurements to include two samples of flesh and two samples of backbone, each taken from separate individuals.

2.3. The method of fundamental solutions

The method of fundamental solutions (MFS) is simply based on a linear superposition of fundamental solutions to approximate the solution of the problem, assuming sources located outside of the computational domain to avoid singularities in the solution. It is based on a collocation approach without requiring any numerical or analytical integration. The MFS has been successfully applied to interpret TS measurements of other large pelagic species, and a complete description of the MFS application to TS calculation can be found in Pérez-Arjona et al. (2020). A short description of the MFS applied to this problem is described below.

The propagation of sound within a homogeneous acoustic space can be mathematically represented in the frequency domain by the Helmholtz differential equation,

$$\nabla^2 p + k^2 p = 0 \tag{2}$$

where $\nabla^2 = \frac{\partial^2}{\partial x^2} + \frac{\partial^2}{\partial y^2} + \frac{\partial^2}{\partial z^2}$ in the case of a 3D problem; p is the acoustic pressure, $k = \frac{\omega}{c}$ the wave number, $\omega = 2\pi f$ the angular frequency, f the frequency and c the sound propagation speed within the acoustic medium.

For the 3D case, assuming a point source placed within the propagation domain, at point $\boldsymbol{x_0}$ with coordinates (x_0, y_0, z_0), it is possible to establish fundamental solutions G, for the sound pressure, and H, for the particle speed, at a point $\boldsymbol{x}$ with coordinates (x, y, z), which can be written respectively as:

$$G^{3D}(x, x_0, k) = \frac{e^{-ikr}}{r} \tag{3}$$

$$H^{3D}(x, x_0, k, \vec{n}) = \frac{1}{-i\rho\omega} \frac{(-ikr - 1)e^{-ikr}}{r^2} \frac{\partial r}{\partial \vec{n}} \tag{4}$$

In these equations, r corresponds to the distance between the source point and the domain point, given; $\vec{n}$ represents the direction along which the particle speed is calculated and ρ the medium density.

To evaluate the main contributions to the scattering properties of fish, we propose a simplified fish model that includes the flesh (designed as medium Ω_2) and backbone (medium Ω_3). Both structures are modelled as fluid filled inclusions, with acoustic properties (c, ρ) values obtained from the results of the experimental measurements described in the previous sections and distinct from the host water medium (Ω_1).

The basic principle of the MFS is that the sound field in a homogeneous region can be simulated by the linear superposition of the effects of a number of virtual sources, each one with its own amplitude, and which must be located outside the domain of interest see (Fairweather et al., 2003). So, to define the formulation of this problem, first it is needed to consider the location of four sets of virtual sources: the first and second on the inner (inside the medium Ω_2) and outer (Ω_1) sides of the flesh-water interface, respectively, each with NS1 sources,; the third (Ω_3) and fourth (Ω_2) on the inner and outer sides of the spine-flesh interface, each with NS2 sources.

The first set will allow the simulation of the sound field in the host medium (Ω_1), which, in that case, can be written as:

$$p(\boldsymbol{x}, k)_{\Omega_1} = \sum_{j=1}^{NS1} P_j G^{3D}(\boldsymbol{x}, \boldsymbol{x}_{1,j}, k_1) + p_{inc}(\boldsymbol{x}, \boldsymbol{x}_{source}, k_1); \ \text{for} \boldsymbol{x} \text{in} \Omega_1 \tag{5}$$

the second and third sets of virtual sources, allow to compute the sound

field within the flesh (Ω_2) as:

$$p(\boldsymbol{x},k)_{\Omega_2} = \sum_{j=1}^{NS1} Q_j G^{3D}(\boldsymbol{x},\boldsymbol{x}_{2,j},k_2) + \sum_{j=1}^{NS2} R_j G^{3D}(\boldsymbol{x},\boldsymbol{x}_{3,j},k_2);\ \text{for}\boldsymbol{x}\text{in}\Omega_2 \tag{6}$$

while within the spine (Ω_3) the acoustic pressure is given as:

$$p(\boldsymbol{x},k)_{\Omega_3} = \sum_{j=1}^{NS2} S_j G^{3D}(\boldsymbol{x},\boldsymbol{x}_{4,j},k_3);\ \text{for}\boldsymbol{x}\text{in}\Omega_3 \tag{7}$$

being P_j, Q_j, R_j and S_j the unknown amplitudes of the virtual sources, $p_{inc}(x, x_{source}, k)$ represents the incident field generated by a source located at x_{source}, and k_i represents the wavenumber in the medium Ω_i. The relevant amplitudes can be determined solving the system of equations established by imposing the necessary continuity of pressure and of normal particle speed in the interface host water-flesh and in the interface flesh-spine (Pérez-Arjona et al., 2018). To establish the formulation of the method, a number of collocation points must be considered throughout the surfaces of the flesh (designed as Γ_1) and of the spine (Γ_2). Imposing the stated boundary conditions at those discrete points homogeneously distributed throughout the two surfaces (points $\overline{x}_{i,\Gamma_1}$ and$\overline{x}_{i,\Gamma_2}$), an equation system with (2xNS1 +2xNS2) equations on (2xNS1 +2xNS2) unknowns can be written as:

$$\mathbf{Ax} = \mathbf{B} \Longleftrightarrow \begin{bmatrix} \mathbf{G}_{G_1,1,\Omega_1} & -\mathbf{G}_{G_1,2,\Omega_2} & -\mathbf{G}_{G_1,3,\Omega_2} & \mathbf{0} \\ \mathbf{H}_{G_1,1,\Omega_1} & -\mathbf{H}_{G_1,2,\Omega_2} & -\mathbf{H}_{G_1,3,\Omega_2} & \mathbf{0} \\ \mathbf{0} & \mathbf{G}_{G_2,2,\Omega_2} & \mathbf{G}_{G_2,3,\Omega_2} & -\mathbf{G}_{G_2,4,\Omega_3} \\ \mathbf{0} & \mathbf{H}_{G_2,2,\Omega_2} & \mathbf{H}_{G_2,3,\Omega_2} & -\mathbf{H}_{G_2,4,\Omega_3} \end{bmatrix} \begin{bmatrix} \mathbf{P} \\ \mathbf{Q} \\ \mathbf{R} \\ \mathbf{S} \end{bmatrix} = \begin{bmatrix} -\mathbf{p}_{inc,\Omega_1} \\ -\mathbf{v}_{inc,\Omega_1} \\ \mathbf{0} \\ \mathbf{0} \end{bmatrix} \tag{8}$$

In Eq. (8), each entry of **A, x and B** corresponds, to a submatrix which contains the effects of each set of virtual sources on each boundary. $\boldsymbol{G}_{G_i j,\Omega_k}$ and $\boldsymbol{H}_{G_i j,\Omega_k}$ are submatrices containing the effect of the virtual sources' j set on boundary Γ_i, considering the properties of the medium Ω_k, in terms of pressure ($\boldsymbol{G}$) or particle velocity ($\boldsymbol{H}$); the right-hand term includes the contribution of the source impinging the scatterer. Solving the assembled equation system, the pressure at any point of the host water domain can be determined making use of Eq. (5). Here, we provide a brief overview of the method applied to the model used in this study. A comprehensive description of the method, including details of each matrix for various case studies, can be found in (Pérez-Arjona et al., 2018).

The computational and precision limit in the results is given by the memory requirements necessary to solve the system (8) and by the condition number associated with matrix A (Golub and Loan, 2013), respectively. With larger fish sizes and higher working frequencies, the dimension of this matrix increases and, therefore, the use of high-performance computing tools is necessary. On the one hand, more powerful computers with fast processors and a high amount of main memory are needed. On the other hand, the use of stable numerical methods is critical to solving large-dimensional equation systems. For the resolution of the system addressed in this work, we propose the QR decomposition method (Golub and Loan, 2013), since it is one of the most stable methods. The resolution process consists of:

- Step 1: Decompose the matrix $A: A = QR$, where Q is an orthogonal matrix and R is an upper triangular matrix.
- Step 2: Solve the upper triangular system: $x = R\backslash(Q^*B)$, where $Q^*$is the adjoint Q matrix.

The memory requirements in the resolution of the system increase considerably since we work in complex arithmetic. Therefore, for larger sizes of fish, methods that perform better management of main memory will be needed in order to be able to obtain valid solutions (Chillarón et al., 2020; Marqués et al., 2009; Quintana-Ortí et al., 2022).

2.4. Application of MFS to target strength calculation of MAC and SKJ models

To perform the MFS model, we adopted simplified geometries for both the fish body and the backbone. In an effort to emphasize the significance of material acoustic parameters when assessing the back-scattered acoustic field, we opted for standard geometries rather than the specific anatomical structures of particular fish species. The body was represented as a prolate spheroid, and the backbone as a straight cylinder with rounded edges to mitigate some of the limitations associated with the MFS model when applied to complex geometries, particularly those featuring sharp edges. As previously mentioned, the measured values of acoustic properties for flesh and backbone tissues were utilized in the acoustic simulation. The dimensions were adjusted to maintain the relative proportions observed in Atlantic mackerel and skipjack tuna (as illustrated in Fig. 2), taking into account not only the fork length but also the transverse size of the fish, which is pertinent to the acoustic backscattering analysis.

The geometry models, labelled as GEOM_SKJ as GEOM_MAC, were tuned to replicate the relative dimensions specific to skipjack tuna (SKJ) and Atlantic mackerel (MAC), using the information from available X-ray images (refer to Fig. 2). To assess the influence of dimensions on each model and the significance of material properties unique to each species, as well as to enable a comparison of the backscattered acoustic field for fish of the same length, both geometries were proportionally scaled to match the dimensions associated with a fish fork length (L) of 25 cm. For that case, flesh was modelled as a prolate spheroid with length, height, and width dimensions: 25, 4.5, and 3.6 *cm* (MAC) and 25, 6.3, and 4.5 *cm* (SKJ). Bone was considered a cylinder with smooth edges with length and diameter dimensions: 22.5, 0.5 *cm* (MAC) and 22.5, 0.6 *cm* (SKJ).

Since the flesh volume and thickness of the backbone of a skipjack tuna are considerably larger than those of an Atlantic mackerel of the same body length, we wanted to determine whether the differences in TS between the two species could be due to dimensional differences or to material properties per se. To evaluate the role of c and ρ on TS independently of the geometry, for each measured pair (c,ρ), both models corresponding to a fish length of 25 cm were run, using different combinations of geometric and material properties, labelled and defined as follows:

i) GEOM_MAC-PROP_MACK: mackerel geometry with (c, ρ) measured for mackerel,
ii) GEOM_MAC-PROP_SKJ: mackerel geometry with (c,ρ) measured for skipjack,
iii) GEOM_SKJ-PROP_SKJ: skipjack geometry with (c,ρ) measured for skipjack, and
iv) GEOM_SKJ-PROP_MAC: skipjack geometry with (c,ρ) measured for mackerel.

The seawater density and sound speed were assumed to be $\rho = 1030\ kg/m^3$ and $c = 1490 m/s$.

The frequency response for mackerel and skipjack and the numerical estimation of the reduced target strength (b_{20}) were addressed using MFS model. The incident acoustic transducer's wave was treated as a plane wave propagating in the positive y-axis direction, emulating the half-beam angle at − 3 dB of 3.5° in line with the specifications of scientific echosounders. It impinged at the dorsal part of the fishes. The Method of Fundamental Solutions (MFS) model was solved at a range of ultrasonic working frequencies: 18, 38, 50, 70, 120, and, when computational resources permitted, 200 kHz. To ensure adequate mesh density, convergence tests were conducted for each frequency. The TS directivity (i.e. relation between TS and fish tilt angle, α) was calculated for dorsal incidence from $\alpha = -90°$ to $\alpha = 90°$ (Fig. 3). The fish-to-transducer distance was fixed to $d = 100\ m$, then lying in the far-field

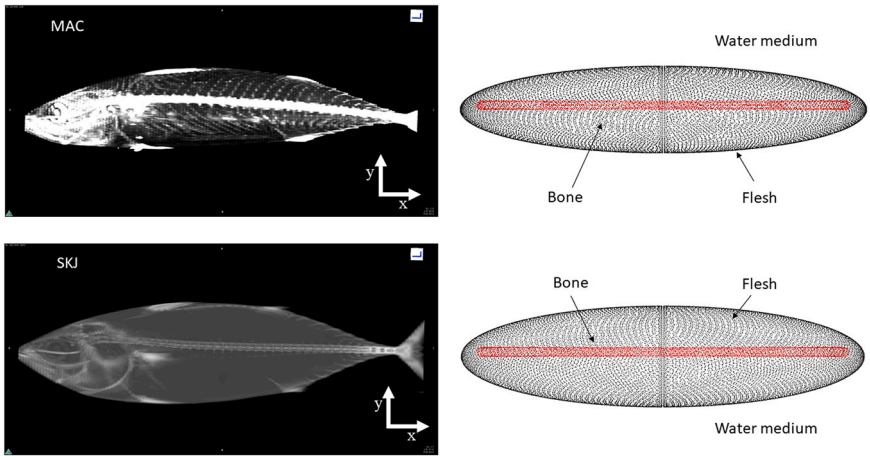

Fig. 2. X -Ray images (Boyra et al., 2018) (left column) and representation of the collocation point distribution in the MFS model of the flesh and backbone (right column) for Atlantic mackerel (upper row) and skipjack tuna (lower row). X-ray images correspond to individuals with length, height, and width dimensions being: 25, 5.3, and 3.9 *cm* (MAC); and 38.1, 10.3, and 7.2 *cm* (SKJ).

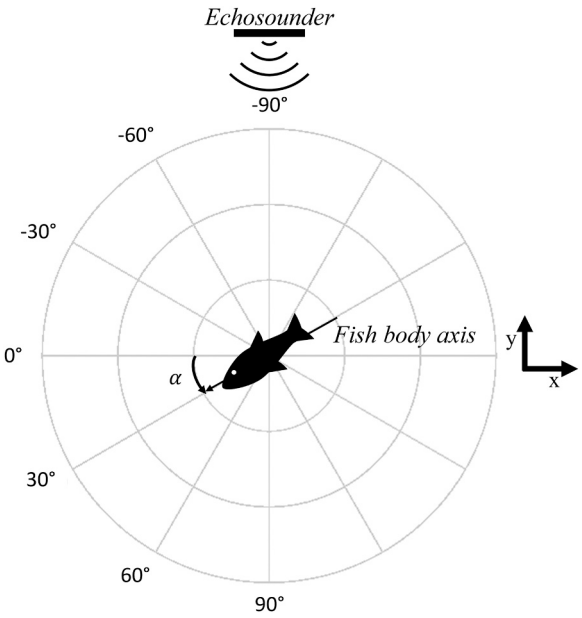

Fig. 3. Scheme of the directivity TS (α) calculation in the x-y plane, being α the tilt angle of fish body axis with respect to the horizontal. The echosounder's emitted beam axis is orthogonal to the fish body axis for $\alpha = 0°$.

region. To consider the same possible fish swimming orientation pattern to both species, TS values were averaged considering a Gaussian weighting function N(0,10) to describe the swimming tilt distribution, centered at $\alpha = 0^o$ with a standard deviation of 10° and defined as TS (0,10) (Forland et al., 2014). In order to evaluate the contribution of each scatter at each working frequency, the numerical simulations were conducted considering: i) backscattering from the body flesh, ii) backscattering from the backbone and iii) backscattering from body flesh and backbone. It should be noted that this method calculates the complete backscattering when the whole fish structure (flesh + backbone), considering also the possible coherent effects. Some previous works (Gorska et al., 2005) considered only the incoherent addition of the backscattered field from backbone and flesh independently.

Finally, for the purpose of comparison with previously reported experimental data, we calculated the TS for the geometry associated with each species, utilizing their respective (c, ρ) measured values, at the common frequencies of 38 kHz and 120 kHz. Subsequently, we determined the corresponding b_{20} parameter for each case (Love, 1971). Following the same procedure as in the experimental campaigns, we considered the fish dimension of our samples extracted from the x-ray images, with length, height, and width dimensions being: 25, 5.3, and 3.9 *cm* for mackerel and 38.1, 10.3, and 7.2 *cm* for skipjack. The TS directivity was calculated for dorsal incidence for relative tilting angle between the fish axis and the beam direction propagation $\alpha = -90°$ up to 90^o. In the case of mackerel, the influence of the swimming direction was included by using the tilt angle distributions reported in Fernandes et al. (2016). Otherwise, for the skipjack, in the absence of swimming distribution data, the general Gaussian function, centered at $\alpha = 0^o$ with a standard deviation of 10° was used to describe the swimming tilt. The b_{20} parameter was obtained for both species for further comparison with reported measured b_{20} values for mackerel (Scoulding et al., 2017), associated with the tilt swimming distribution (Fernandes et al., 2016), and with in-situ and *ex-situ* measurements for skipjack (Boyra et al., 2018; Oshima, 2008), respectively.

3. Results

3.1. Validation of sound speed measurement set-up and time response calibration

To validate the method, we measured the speed of sound in water by the linear relationship of the distance between transducers and the flying time. The slope of the regression line obtained from the experimental measurements was the sound speed in the medium (Fig. 4). The obtained sound speed in fresh water was $c = 1503(6)m/s$, which was in good agreement with the predicted value $1498.0(0.7)m/s$ (from Lubbers and Graaff's equation at 25.3 ^oC). In the following, values in parentheses correspond to the standard deviation of the magnitude, which provides an estimation of the accuracy of the results.

The intercept (b) value in the experimental linear fit is related with the response time (t_R) of the system – theoretically the intercept is null-being $t_R = b/c$. The response time, to be further used, was found to be $t_R = 19.9(0.3)\mu s$.

3.2. Sound speed measurement in Atlantic mackerel and skipjack tuna flesh

To measure sound speed on Atlantic mackerel and skipjack tuna flesh samples, the relation between the distance d between transducers and the acoustic pulse flight-time $t = t_F - t_R$ (which includes the response time of the system), was considered.

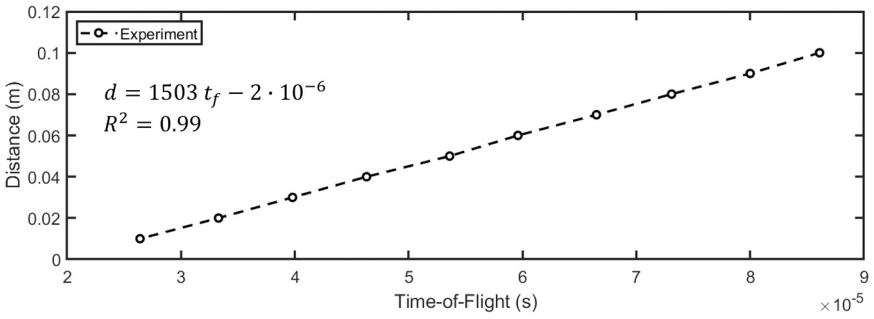

Fig. 4. Linear relationship of the distance between transducers and the time of flight to calibrate the measurement of the speed of sound in water: experimental result correcting the time response (dashed line). The x-axis indicates the measurement of the Time-of-Flight and the y-axis the measurement of the distance between the transducers.

The obtained value of sound speed for Atlantic mackerel flesh was $c_{fl,MAC} = 1520(90)m/s$, with $R^2 = 0.97$. In the case of skipjack tuna flesh (R^2 =0.99), the measured sound speed was higher than for Atlantic mackerel flesh, being $c_{fl,SKJ} = 1680(10)m/s$ (Fig. 5).

3.3. Sound speed measurement in Atlantic mackerel and skipjack tuna backbone

The sound speed measurements for a 15 mm-long sample of Atlantic mackerel backbone were estimated based on 12 measurements (refer to Table 1). These measurements involved changing the backbone's orientation and position, taking into consideration the measurement's dispersion error. The obtained speed value was $c_{bone,MAC} = 2200(200)m/s$.

To obtain an average value of c in skipjack backbone, also 12 measurements were performed on a tuna's backbone tuna sample (Table 1). The result reveals that the measured sound speed in skipjack backbone was $c_{bone,SKJ} = 3530(160)m/s$, being higher than Atlantic mackerel's.

As has been reported for other species, and as it is the case for Atlantic mackerel, the results show a large variability of sound speed in skipjack backbones, depending on the sample. To avoid the backbone characteristics changing with time (e.g. by losing humidity), the measurements were not repeated with the same backbone sample in

Table 1
Sound speed obtained for Atlantic mackerel and skipjack tuna backbone: $c_{backbone}$ is for the mean value and std for standard deviation.

Sound velocity backbone (m/s)		
Measurement	MAC	SKJ
1	2500	3779
2	2458	3583
3	1859	3779
4	2118	3416
5	2382	3416
6	2276	3373
7	2279	3664
8	1950	3416
9	2210	3664
10	2370	3596
11	2035	3370
12	2479	3342
$c_{backbone}$	2200	3530
std	200	160

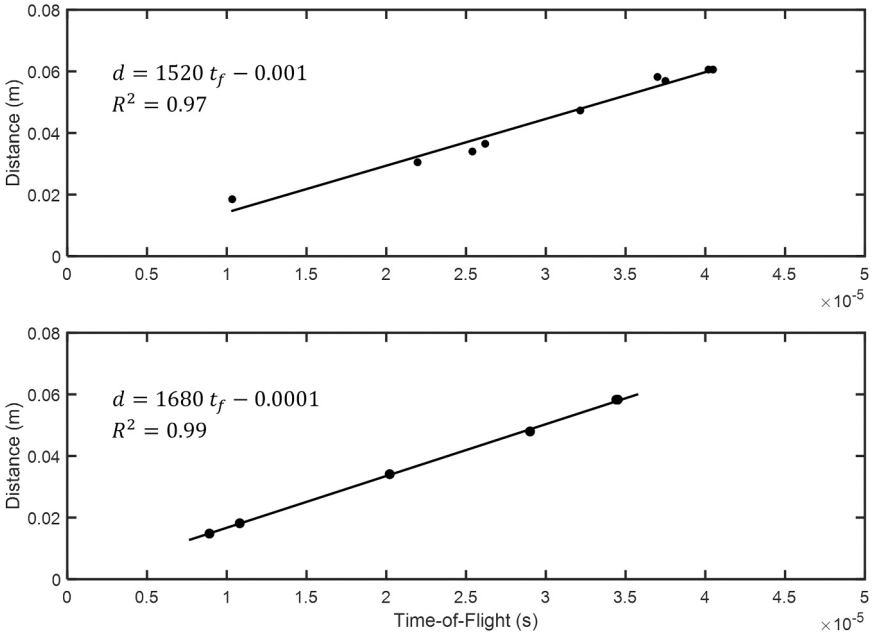

Fig. 5. Linear adjustment between flying time and distance between transducers for Atlantic mackerel (panel upper) and skipjack tuna (panel lower). On the x-axis is the measured time of flight and on the y-axis is the measured distance of the transducers.

different sessions.

3.4. Volumetric mass density measurements

The density measurements for Atlantic mackerel and skipjack tuna tissues were conducted on the same samples used for measuring the ultrasonic sound speed. The results for the volumetric density measured on mackerel were 1060(40) kg/m^3 and 1090(20) kg/m^3, for flesh and backbone, respectively. Higher values were obtained for skipjack, being 1090(40)kg/m^3 for flesh and 1230(30)kg/m^3 for backbone.

3.5. Numerical estimation of TS for Atlantic mackerel and skipjack tuna models

3.5.1. Relevance of the acoustic parameter values and the geometric model on TS

The TS (0,90) was numerically estimated for the geometries for mackerel and skipjack, labelled respectively GEOM_MAC and GEOM_SKJ, scaled for a fish length of L= 25cm. To evaluate the role of the acoustic parameters we have considered the measured (c,ρ) pairs for each species applied also to the geometry of the other one. The TS frequency response was different for each geometry, and, for the same geometry, the absolute value of TS(0,90) was higher when we considered the (c,ρ) values for skipjack than for mackerel. Nevertheless, the trends of the frequency response curve were linked to the geometry of the model: to evaluate the same geometry with different (c,ρ) provides almost parallel frequency response curves (Fig. 6). At the evaluated frequencies (18, 38, 50, 70, 120 and 200 kHz), the mackerel geometry exhibited a noteworthy minimum at 38 kHz, which was not observed in the skipjack geometry. As the frequency increased, beyond 70 kHz, models employing identical (c, ρ) values generated similar TS values for both geometries. This similarity intensified at higher frequencies. At 200 kHz, when the (c, ρ) values for skipjack were applied, the TS(0,90) was − 40.2 dB for SKJ_GEOM and − 40.6 dB for MAC_GEOM. In the case of mackerel (c, ρ) values, TS recorded − 44.2 dB for SKJ_GEOM and − 45.7 dB for MAC_GEOM (as shown in Fig. 6). Notably, differences exceeding 4 dB were observed when the same geometry was utilized with the material properties of skipjack compared to those of mackerel.

3.5.2. Relative contribution to backscattering of each scatter for SKJ and MAC models

The frequency dependence of TS was considered for the different structures: only flesh (F-model), only the backbone (B-model) and flesh plus backbone (F&B-model), to interpret their contribution to the backscattered field. The far-field directivities, TS versus α, for each model and for both species was calculated at 38 and 120 kHz for a 25 cm fish length (Fig. 7). From those TS directivities, TS(0,10) was developed and considered to evaluate the role of each scatter.

As expected, in the case of Atlantic mackerel flesh, the acoustic contrast with the seawater is low and consequently, for higher frequencies, over 70 kHz, the backscattering is mainly ruled by the backbone being the TS(0,10) for the F&B-model (−47.8 dB) the same than for the B-model (−47.2 dB) (Fig. 8). Nevertheless, in the case of the skipjack tuna, although, observing that also the contribution of the backbone to the scattered field increases with the frequency, the TS (0,10) values given by the F&B-model and by the B-model are not equivalent, being almost 4 dB larger for latter one (Fig. 8).

3.5.3. Numerical estimation of b_{20} parameter

We evaluated the b_{20} parameter for the two species under study considering the previously measured acoustic parameters and the reported, when existing, swimming tilt distribution. We chose (Fernandes et al., 2016) to describe the mackerel swimming distribution. In the absence of further information, for describing the swimming titling of skipjack we chosen a general Gaussian distribution N(0,10). Nevertheless, it should be remarked that the same distribution used for mackerel was also applied to the skipjack results, with no relevant differences respect to the results reported here.

The b_{20} parameter for mackerel was − 90 dB and − 84.3 at 38 and 120 kHz, respectively. For the skipjack, the obtained value for b_{20} was − 74.6 dB (38 kHz) and − 70.8 dB (120 kHz). Differences exceeding 10 dB, with the skipjack case exhibiting a greater difference compared to mackerel, were observed at both frequencies (Table 2).

4. Discussion

The acoustic properties of the constituent materials within fish anatomy play a pivotal role in governing the backscattering of acoustic energy when a fish is exposed to an ultrasonic beam. As a result, the measured TS is significantly influenced by these properties, with particular emphasis on the roles of flesh and backbone, which become even more critical for swimbladderless species.

To characterize accurately the acoustic response of a target fish, it is essential to possess information about its external and internal geometry, its composition in terms of its various tissues, and the corresponding values of longitudinal sound speed (c) and mass density (ρ). These acoustic parameters are species-specific and may even vary within the same species based on factors such as fat content, which is contingent upon sex, size, season, or geographical location of the specimen (Sigfusson et al., 2001).

We characterized the acoustic impedance of skipjack tuna tissues, both flesh and backbone, and compared it with that of Atlantic mackerel. This involved measuring the sound speed at 120 kHz, a common working frequency for echosounders and Fish Aggregating Devices (FADs). The objective was to obtain realistic acoustic parameter values for use in numerical models. These models help in the interpretation of experimental data and provide insights into the reported differences between the two species (Boyra et al., 2018; Oshima, 2008; Scoulding et al., 2017). We have summarized the general results for the two species

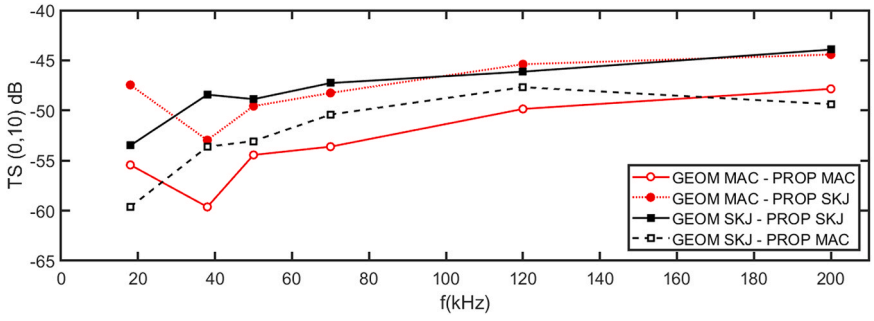

Fig. 6. TS (0°,10°) values at 18, 38, 50, 70, 120 and 200 kHz, for Atlantic mackerel (MAC) and skipjack tuna (SKJ) models with fish length= 25cm. The following acoustic simulation models have been considered: MAC model geometry and acoustic properties of MAC tissues (solid line red), MAC model geometry and SKJ properties (dash-dotted line red), SKJ model geometry and SKJ properties (solid line black) and SKJ model geometry and MAC properties (dashed line black).

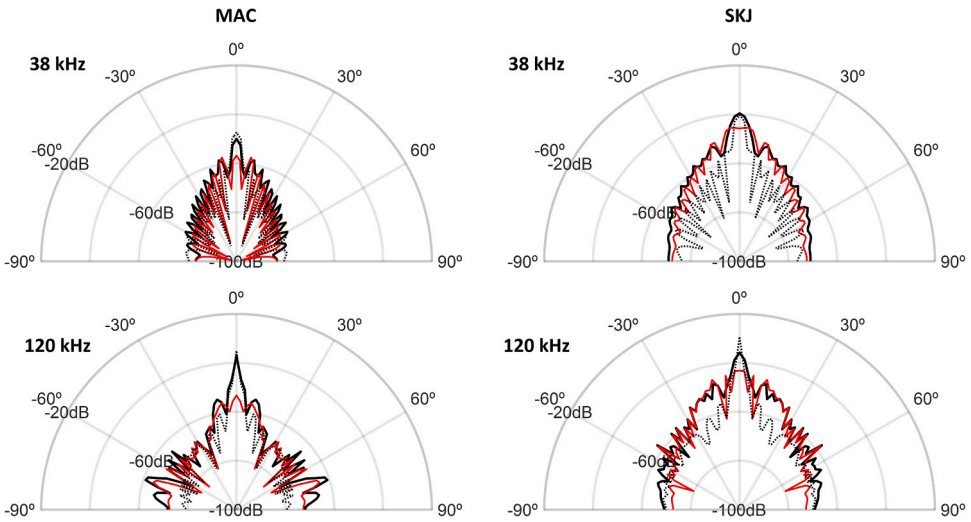

Fig. 7. TS (α) versus fish orientation angle α for 38 kHz (panel upper) and 120 kHz (panel lower) for Atlantic mackerel (left column) and skipjack tuna (right column) with fish length 25 cm considering the model of body flesh (solid line red), the model backbone (dash-dotted line black) and the model of body flesh plus backbone (solid line black).

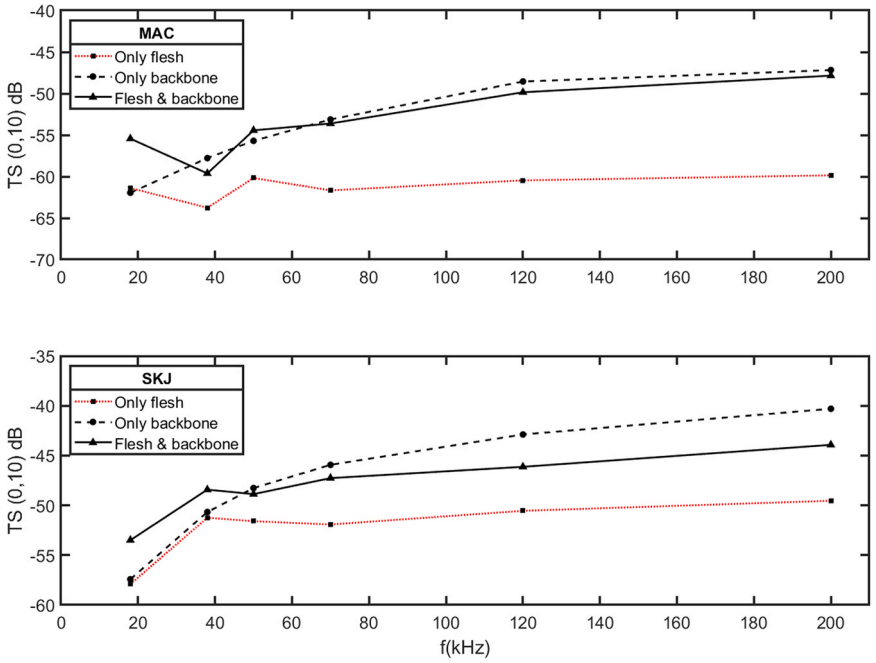

Fig. 8. TS (0°,10°) at 18, 38, 50, 70, 120 and 200 kHz, for Atlantic mackerel (panel upper) and skipjack tuna (panel lower) models with fish length= 25cm. Only flesh (dash-dotted line red), only backbone (dashed line) and flesh plus backbone (solid line back) had been considered.

Table 2
Summary of material properties for Atlantic mackerel and skipjack tuna tissues. Mean and standard deviation (std) values are indicated.

Parameters		MAC		SKJ	
		Flesh	Backbone	Flesh	Backbone
c(m/s)	*mean*	1520	2200	1680	3530
	std	90	200	10	160
ρ(kg/ m^3)	*mean*	1060	1090	1090	1230
	std	40	20	40	30
z (kg s^{-1} m^{-2})	*mean*	$1.61{\cdot}10^6$	$2.4{\cdot}10^6$	$1.83{\cdot}10^6$	$4.3{\cdot}10^6$
	std	$0.06{\cdot}10^6$	$0.2{\cdot}10^6$	$0.07{\cdot}10^6$	$0.2{\cdot}10^6$

(Table 2). The obtained value of sound speed for Atlantic mackerel flesh was $c_{fl,MAC} = 1520m/s$, in good agreement with the previous results in (Gorska et al., 2005, 2007), were sound-speed contrast of 1.025 was reported, and in (Sigfusson et al., 2001), where sound speed contrast was given by the expression 1.034–0.125 F, being F the Atlantic mackerel fat content.

The sound speed was notably higher for skipjack tissues, both for the backbone and the flesh. The sound speed value obtained for skipjack flesh, $c_{fl,SKJ} = 1680m/s$, is similar and even slightly higher than previously reported c values for other tuna species at higher working frequencies (Shibata, 1970; Sigfusson et al., 2001). The sound speed seems to be nearly independent of the working frequency in most cases. However, previous studies have reported frequency dispersion of sound velocity in human tissues (Wear, 2000), making it relevant to measure

the backbone sound speed at working frequencies close to the echosounder's. For the sake of coherence, we measured all tissues at the same frequency. The notable difference in tissue impedance between skipjack tuna and Atlantic mackerel is particularly significant when interpreting their target strength (TS), especially considering the absence of swimbladder in both species.

The lack of information on the values of these parameters for most of the species has been pointed out in previous works, even for well-known species as Atlantic mackerel (Gorska et al., 2007). Atlantic mackerel is one of the best characterized species from the acoustical point of view and it is considered a paradigm of fish that do not have swimbladder (Forland et al., 2014; Gorska et al., 2005). Therefore, the acoustic backscattering of other fish species without swimbladder is usually compared with the expected backscattering of Atlantic mackerel. However, as previously mentioned, for a comprehensive interpretation of acoustic results concerning a specific species, it is necessary to possess knowledge of the acoustic properties of its tissues. When the sound speed and mass density values of one species are used to analyze data from a different species (e.g., interpreting skipjack tuna data using the acoustic properties of Atlantic mackerel), it may lead to overestimation or underestimation of the acoustic response. In the context of our study, it is important to note that skipjack tissues exhibited a significantly higher acoustic impedance compared to mackerel: 14 % for flesh and 79 % for backbone (Table 2).

In our measurements, we observed that the dispersion of sound speed in mackerel bone was relatively larger (28 %) compared to skipjack, where the dispersion was 11 %. Our findings align well with previous data from (Gorska et al., 2005, 2007), which reported a sound-speed contrast of 1.3–2.0 (equating to 1950–3000 m/s) for compressional waves in fish backbones. It is worth noting that (Gorska et al., 2005, 2007) did not provide sound speed measurements for Atlantic mackerel backbone, explicitly highlighting the lack of information on this aspect in their study.

As previously mentioned, c and ρ are subject to variations based on various factors, even within the same species. Therefore, it is essential to interpret the measured values (refer to Table 2) within this broader context. While more extensive measurements are needed to characterize material properties across fish size, age, sex, or fat content, the presented results contribute to an enhanced understanding of the acoustic properties specific to skipjack and mackerel tissues, as well as the differences between these two species.

These data offer valuable insights for species identification, serving as a resource for numerical modeling and aiding in the interpretation of experimental data acquired from mackerel and skipjack in situ (Moreno et al., 2019).

We conducted a comparative analysis of the influence of acoustic impedance (z) and model geometry (specifically, differences in flesh volume and bone thickness) on target strength (TS) for both species. Higher z values are associated with increased backscattered acoustic intensity and, consequently, higher TS values, regardless of the chosen geometry.

The significance of material property values and model geometry is further elucidated through the assessment of the TS frequency response. Two key points should be emphasized. Firstly, the geometry plays a dominant role in shaping the characteristics of the TS frequency response curve, independently of the (c, ρ) values employed in the calculations (Fig. 6).

Regarding the characteristics of the target strength (TS) vs. frequency curve, a noteworthy feature is the dip observed around 38 kHz when the mackerel's geometry was considered. The presence of such dips in the frequency response holds promise as a valuable tool for remote species identification and was previously reported for mackerel (Korneliussen, 2010). It is important to note that reproducing experimental data demands careful consideration of additional factors, including anatomy, size, and swimming distribution patterns. Therefore, the results may not be directly comparable. However, the agreement regarding the presence of this specific type of dip emphasizes its significance for future species' identification studies. Secondly, as the frequency increases above 70 kHz, the absolute value of TS for each frequency depends on the (c, ρ) values but not on the geometry: the same value of TS was obtained for different geometries, considering the same (c, ρ) (Fig. 6).

The calculations performed for each species geometry, using for each species its own measured tissue properties, confirmed the experimental results (Boyra et al., 2018). As expected, owing to the larger volume of the target and the higher acoustic impedance of the tissues, the modeled TS was consistently higher for skipjack compared to mackerel. This difference was observed for fish of the same length (L=25 cm) at each working frequency (Fig. 8).

The relative contributions of the two scattering structures considered, fish flesh and backbone, to the acoustic backscattering varied with the specific acoustic parameter values. As expected, the contribution of fish bone to the backscattering became more significant as the frequency increased. The directivity of bone's contribution also grew more pronounced at tilt angles close to 0°. This implies that tilt-averaged target strength depends on the chosen swim tilt distribution and that this dependence becomes more marked at higher frequencies due to increased directivity. Enhancing our understanding of the tilt distribution of free-swimming fish in situ is essential for providing a more accurate description of the measured TS for each species. To facilitate a comparison across different species, all results were initially calculated considering a Gaussian distribution N(0,10).

At higher frequencies, for mackerel, the backscattered field was primarily dominated by the bone (as shown in Fig. 8), making the TS calculated for the entire flesh and bone (F&B) model essentially equivalent to the TS calculated for the bone model (Gorska et al., 2007). In the case of skipjack, a similar trend was observed, but the TS from the F&B model and the bone model were not equivalent. This discrepancy was influenced by the higher acoustic impedance of skipjack flesh, which caused a reduction in the intensity of the sound wave reaching the bone, resulting from a shadowing effect. This effect led to lower TS obtained from the F&B model in comparison to the bone model. Importantly, this phenomenon is not solely attributable to the chosen swimming pattern for averaging TS and can be observed even for the 0° direction (see Fig. 7). Therefore, the relationship of (c, ρ) values between flesh and

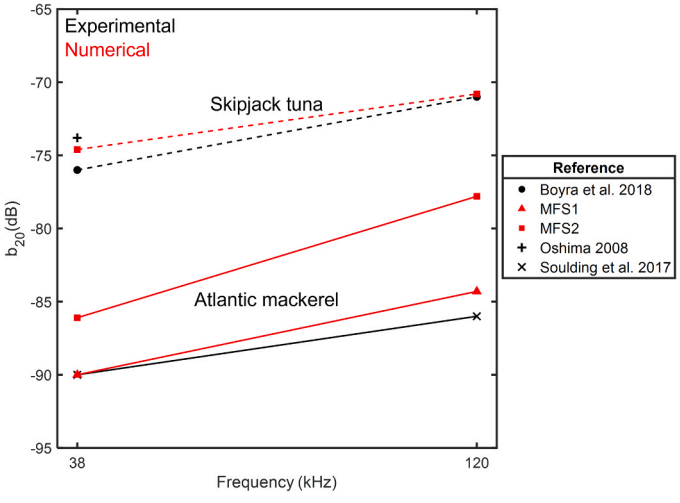

Fig. 9. Comparison of the numerically (red) calculated b_{20} parameter with previously reported b_{20} from experimental data (black) at two typical acoustic frequencies. For Atlantic mackerel (continuous line), the swim tilt distribution for the simulation was obtained either from Fernandes et al. (2016) (MFS1) or using a N(0,10) distribution (MFS2); for skipjack tuna (dashed line), as no published values were available, only the N(0, 10) distribution was considered (i.e. MFS2).

backbone within a given species significantly alters their relative contributions to the total dorsal backscattering of the fish. Previous experimental studies have reported variations in the b_{20} parameter obtained for two species: skipjack and mackerel (see Fig. 9). These discrepancies can be attributed to a wide range of factors, including, but not limited to, differences in their internal anatomy and external shape, acoustic data acquisition and processing methods, and the swimming distribution of these fish. In this study, we compare the estimated b_{20} values, using the best-known swimming distribution available for mackerel, as provided by Fernandes et al. (2016), with a Gaussian N(0,10) distribution for skipjack, to the measured b_{20} values for both mackerel and skipjack (Boyra et al., 2018; Oshima, 2008).

To assess the influence of fish behavior, we also calculated b_{20} for mackerel using a Gaussian N(0,10) distribution as the swimming pattern. The results revealed an approximate 4 dB increase compared to the values obtained using the swimming pattern reported in Fernandes et al. (2016): − 86.1 dB compared to − 90 dB at 38 kHz and − 77.8 dB compared to − 84.3 dB at 120 kHz, respectively. This increase can be attributed to the maximum backscattered field observed at $\alpha = 0°$, as shown in Fig. 7,which is linked to the model symmetry, and the significant contribution of this tilting direction to the average backscattering for the N(0,10) swimming pattern. These differences in the b_{20} values highlight the significance of fish behavior in interpreting acoustic data.

When using the swimming behavior data from Fernandes et al. (2016) for mackerel, our simulations produced b_{20} values at 38 kHz and 120 kHz (Fig. 9) that closely matched the experimental values reported in Scoulding et al. (2017). At 38 kHz, both simulation and experiment yielded nearly identical results (−90 dB). However, at 120 kHz, the simulation slightly exceeded the experimental value (−84.3 dB compared to −86 dB). In the case of skipjack, our simulated b_{20} values exceeded those of mackerel by more than 10 dB, in line with experimental data (Fig. 9). At 38 kHz, the numerical estimations closely aligned with the experimental values: b_{20}= −74.6 dB compared to − 76 dB and − 73.8 dB from Boyra et al. (2018) and Oshima (2008), respectively. At 120 kHz, the experimental b_{20} (−71 dB) slightly exceeded the simulated result (−70.8 dB) obtained by Boyra et al. (2018). These findings highlight the significance of the knowledge regarding the acoustic properties of fish tissues for each species, aiding in the interpretation of simulated target strength (TS) values. It underscores the value of incorporating these material properties into numerical models.

While this study enhances our understanding of fish species' material properties and their role in acoustically identifying and distinguishing fish without a swimbladder, it is important to acknowledge its limitations. The main limitation was that the results were based on experiments with a limited sample size. Therefore, conducting further experiments to explore intraspecific variability and increase the precision of the obtained values is advisable.

The model used in this study employed simplified geometries, assuming the backbone to be a straight cylinder and the flesh to be a prolate spheroid. The purpose was to investigate the role of acoustic parameters in contributing to target strength (TS) and to understand how differences in these parameters could independently influence TS, without considering other contributions. This model did not encompass all the scattering elements found in fish anatomy. To replicate accurately the complete backscattering of fish, a more detailed and realistic fish geometry should be considered for each species. This should involve incorporating precise flesh shapes, accounting for the relative orientation between the fish axis and the spine/backbone, considering the modulation of spine vertebrae, and including other scattering elements such as the skull, guts, or gills. Regarding the backbone, its curvature has been shown to be relevant to TS directivity, and its modulation can alter the TS directivity pattern, even introducing grating lobes. These grating lobes have been observed in measurements (Nesse et al., 2009) and predicted numerically (Pérez-Arjona et al., 2020). As the complexity of the model increases, a balance between model detail and computational requirements becomes crucial. For instance, modeling the fish's skull demands considerable computational resources, but its contribution is less significant for swimming tilt angles near 0° (Forland et al., 2014). Increasing our understanding of the swimming direction of the fish school is essential when comparing numerical estimates with data from acoustic surveys. This is due to the fish's directivity, which becomes more pronounced at higher frequencies, such as 120 kHz (as seen in Fig. 7). The complexity of the directivity pattern also grows as more realistic geometries are considered, making swimming tilt information increasingly vital for accurate models. Other sources of variability affecting target strength (TS), such as the fish's condition factor, size, gender distribution within the school, and natural variations among individuals, are challenging to address through numerical models. Their influence should be evaluated when comparing results with experimental data. Other sources of variability affecting TS, as the condition factor of the fish, size, and gender distribution in the school and natural variability among individuals are difficult to address through numerical models and their influence should be evaluated when compared with experimental results.

5. Conclusions

This study focuses on the differences in target strength (TS) and frequency response between two swimbladderless fish species. We conducted new measurements of flesh and backbone density and sound speed for skipjack tuna and Atlantic mackerel. The experimental measurements of Atlantic mackerel flesh were consistent with previously published data, validating our methodology. We used these newly obtained material properties to perform backscattering simulations using the Method of Fundamental Solutions. These simulations helped us understand the acoustic properties of both species at relevant frequencies. The differences in impedance accounted for the TS variations between species for every single frequency, while variations in geometry (larger flesh volume and bone thickness in skipjack for the same body length) predicted differences in frequency response, particularly at lower frequencies. These results evidence the qualitative and quantitative importance of fish tissue acoustic impedance (flesh and backbone) in numerical TS estimation for swimbladderless species. Future experimental efforts are needed to provide acoustic characteristics of fish tissues, particularly for commercially significant species lacking swimbladders, which are frequently subject to stock assessments. These measured TS values can be interpreted more effectively with more extensive information on the acoustic properties of fish tissues.

CRediT authorship contribution statement

A. Ladino: Methodology, Software, Investigation, Writing – original draft, Visualization. **I. Pérez-Arjona:** Methodology, Conceptualization, Software, Investigation, Writing – original draft, Visualization, Writing – review & editing, Supervision, Project administration, Funding acquisition. **V. Espinosa:** Methodology, Conceptualization, Investigation, Writing – review & editing. **M. Chillarón:** Software, Investigation, Validation. **V. Vidal:** Software, Investigation, Validation. **L.M. Godinho:** Software, Methodology. **G. Moreno:** Conceptualization, Resources, Funding acquisition. **G. Boyra:** Conceptualization, Writing – review & editing.

Declaration of Competing Interest

The authors declare that they have no known competing financial interests or personal relationships that could have appeared to influence the work reported in this paper.

Data Availability

Data will be made available on request.

Acknowledgements

This work was funded by MCIN/AEI/10.13039/501100011033/FEDER through the ACTHHUN project ref. PID2021-127426OB-C21 and by the International Seafood Sustainability Foundation (ISSF) and conducted independently by the authors. G. Moreno acknowledges the received funding under award NA19NMF4720214 from the 2019 Bycatch Reduction Engineering Program from National Oceanic and Atmospheric Administration (NOAA). Funding for open access charge: MCIN/AEI/10.13039/501100011033/FEDER and Universitat Politècnica de València.

References

Andreeva, I., 1964. Scattering of sound by air bladders of fish in deep sound-scattering ocean layers. Sov. Phys. -Acoust. 10, 17–20 https://doi.org/10003864529.

Boyra, G., Moreno, G., Sobradillo, B., Pérez-Arjona, I., Sancristobal, I., Demer, D.A., 2018. Target strength of skipjack tuna (Katsuwanus pelamis) associated with fish aggregating devices (FADs). ICES J. Mar. Sci. 75 (5), 1790–1802. https://doi.org/10.1093/icesjms/fsy041.

Chillarón, M., Quintana-Ortí, G., Vidal, V., Verdú, G., 2020. Computed tomography medical image reconstruction on affordable equipment by using Out-Of-Core techniques. Comput. Methods Prog. Biomed. 193 (105488), 105488 https://doi.org/10.1016/j.cmpb.2020.105488.

Chu, D., Foote, K.G., Stanton, T.K., 1993. Further analysis of target strength measurements of Antarctic krill at 38 and 120 kHz: comparison with deformed cylinder model and inference of orientation distribution. J. Acoust. Soc. Am. 93 (5), 2985–2988. https://doi.org/10.1121/1.405818.

Clay, C.S., Home, J.K., 1994. Acoustic models of fish: the Atlantic cod (Gadus morhua). J. Acoust. Soc. Am. 96 (3), 1661–1668. https://doi.org/10.1121/1.410245.

Fairweather, G., Karageorghis, A., Martin, P.A., 2003. The method of fundamental solutions for scattering and radiation problems. Eng. Anal. Bound. Elem. 27 (7), 759–769. https://doi.org/10.1016/S0955-7997(03)00017-1.

Fernandes, P.G., Copland, P., Garcia, R., Nicosevici, T., Scoulding, B., 2016. Additional evidence for fisheries acoustics: small cameras and angling gear provide tilt angle distributions and other relevant data for mackerel surveys. ICES J. Mar. Sci. 73 (8), 2009–2019. https://doi.org/10.1093/icesjms/fsw091.

Forland, T.N., Hobæk, H., Ona, E., Korneliussen, R.J., 2014. Broad bandwidth acoustic backscattering from sandeel—measurements and finite element simulations. ICES J. Mar. Sci. 71 (7), 1894–1903. https://doi.org/10.1093/icesjms/fsu010.

Forland, T.N., Hobæk, H., Korneliussen, R.J., 2014. Scattering properties of Atlantic mackerel over a wide frequency range. ICES J. Mar. Sci. 71 (7), 1904–1912. https://doi.org/10.1093/icesjms/fsu045.

Furusawa, M., 1988. Prolate spheroidal models for predicting general trends of fish target strength. J. Acoust. Soc. Jpn. E 9 (1), 13–24. https://doi.org/10.1250/AST.9.13.

Golub, G., Loan, C. van, 2013. Matrix Computations. JHU Press.

González, J.D., Blanc, S.B., Prario, I., Madirolas, A., 2013. Modelling the fish acoustic response: application to laboratory essays on perch (Percicthys trucha). An. AFA 23 (1), 92–101. https://doi.org/10.31527/ANALESAFA.2013.23.1.88.

Gorska, N., Ona, E., Korneliussen, R., 2005. Acoustic backscattering by Atlantic mackerel as being representative of fish that lack a swimbladder. Backscattering by individual fish. ICES J. Mar. Sci. 62 (5), 984–995. https://doi.org/10.1016/j.icesjms.2005.03.010.

Gorska, N., Korneliussen, R.J., Ona Gorska, E., Gorska, N., Korneliussen, R.J., Ona, E., 2007. Acoustic backscatter by schools of adult Atlantic mackerel. ICES J. Mar. Sci. 64 (6), 1145–1151. https://doi.org/10.1093/icesjms/fsm094.

Jech, J.M., Horne, J.K., Chu, D., Demer, D. a, Francis, D.T.I., Gorska, N., Jones, B., Lavery, A.C., Stanton, T.K., Macaulay, G.J., Reeder, D.B., Sawada, K., 2015. Comparisons among ten models of acoustic backscattering used in aquatic ecosystem research. J. Acoust. Soc. Am. 138 (6), 3742–3764. https://doi.org/10.1121/1.4937607.

Kloser, R.J., Horne, J.K., 2003. Characterizing uncertainty in target-strength measurements of a deepwater fish: orange roughy (Hoplostethus atlanticus). ICES J. Mar. Sci. 60 (3), 516–523. https://doi.org/10.1016/S1054-3139(03)00048-1.

Kloser, R.J., Ryan, T., Sakov, P., Williams, A., Koslow, J.A., 2002. Species identification in deep water using multiple acoustic frequencies. Can. J. Fish. Aquat. Sci. 59 (6), 1065–1077. https://doi.org/10.1139/f02-076.

Korneliussen, R.J., 2010. The acoustic identification of Atlantic mackerel. ICES J. Mar. Sci. Volume 67 (Issue 8), 1749–1758. https://doi.org/10.1093/icesjms/fsq052.

Love, R.H., 1971. Dorsal-Aspect target strength of an individual fish. J. Acoust. Soc. Am. 49, 816. https://doi.org/10.1121/1.1912422.

Lubbers, J., Graaff, R., 1998. A simple and accurate formula for the sound velocity in water. Ultrasound Med. Biol. 24 (7), 1065–1068. https://doi.org/10.1016/S0301-5629(98)00091-X.

Macaulay, G.J., Peña, H., Fässler, S.M.M., Pedersen, G., Ona, E., 2013. Accuracy of the Kirchhoff-approximation and Kirchhoff-Ray-Mode fish swimbladder acoustic scattering models. PLoS One 8 (5). https://doi.org/10.1371/journal.pone.0064055.

Marqués, M., Quintana-Ortí, G., Quintana-Ortí, E.S., van de Geijn, R., 2009. Out-of-core computation of the QR factorization on multi-core processors. *Lect. Notes Comput. Sci. (Incl. Subser. Lect. Notes Artif. Intell. Lect. Notes Bioinforma.)*, *5704 LNCS* 809–820. https://doi.org/10.1007/978-3-642-03869-3_75.

Moreno, G., Boyra, G., Sancristobal, I., Itano, D., Restrepo, V., 2019. Towards acoustic discrimination of tropical tuna associated with Fish Aggregating Devices. PLOS ONE 14 (6), e0216353. https://doi.org/10.1371/journal.pone.0216353.

Nesse, T.L., Hobæk, H., Korneliussen, R.J., 2009. Measurements of acoustic-scattering spectra from the whole and parts of Atlantic mackerel. ICES J. Mar. Sci. 66 (6), 1169–1175. https://doi.org/10.1093/icesjms/fsp087.

Nordt III, P.N., Hill, W.C., Rohr, K.L., & Nordt Co. Inc., J.C., 1999. Practical applications of specific gravity determination to platinum jewelry manufacturing. The uses and limitations of Archimedes Principle (Vol. 3, pp. 38–47).

Oshima, T., 2008. Target strength of Bigeye, Yellowfin and Skipjack measured by split beam echo sounder in a cage. IOTC, WPTT-22, 4, 1–4.

Pérez-Arjona, I., Godinho, L.M.C., Espinosa, V., 2018. Numerical simulation of target strength measurements from near to far field of fish using the method of fundamental solutions. Acta Acust. U. Acust. 104 (1), 25–38. https://doi.org/10.3813/AAA.919142.

Pérez-Arjona, I., Godinho, L., Espinosa, V., 2020. Influence of fish backbone model geometrical features on the numerical target strength of swimbladdered fish. ICES J. Mar. Sci. 77 (7–8), 2870–2881. https://doi.org/10.1093/icesjms/fsaa160.

Prario, I.S., Gonzalez, J.D., Madirolas, A., Blanc, S., 2015. A prolate spheroidal approach for fish target strength estimation: Modeling and measurements. Acta Acust. U. Acust. 101 (5), 928–940. https://doi.org/10.3813/AAA.918888.

Puig-Pons, V., Muñoz-Benavent, P., Pérez-Arjona, I., Ladino, A., Llorens-Escrich, S., Andreu-García, G., Valiente-González, J.M., Atienza-Vanacloig, V., Ordóñez-Cebrián, P., Pastor-Gimeno, J.I., Espinosa, V., 2022. Estimation of Bluefin Tuna (Thunnus thynnus) mean length in sea cages by acoustical means. Appl. Acoust. 197 https://doi.org/10.1016/j.apacoust.2022.108960.

Quintana-Ortí, G., Chillarón, M., Vidal, V., Verdú, G., 2022. High-performance reconstruction of CT medical images by using out-of-core methods in GPU. Comput. Methods Prog. Biomed. 218 https://doi.org/10.1016/j.cmpb.2022.106725.

Scoulding, B., Gastauer, S., MacLennan, D.N., Fässler, S.M.M., Copland, P., Fernandes, P. G., 2017. Effects of variable mean target strength on estimates of abundance: the case of Atlantic mackerel (Scomber scombrus). ICES J. Mar. Sci. 74 (3), 822–831. https://doi.org/10.1093/icesjms/fsw212.

Shibata, K., 1970. Study on Details of Ultrasonic Reflection from Individual Fish, Vol. 29. Bulletin of the Faculty of Fisheries, Nagasaki University, pp. 1–82.

Sigfusson, H., Decker, E.A., Morrissey, M., Mcclements, D.J., Sigfusson, H., Decker, E.A., Morrissey, M., Mcclements, D.J., 2001. Ultrasonic characterization of North Pacific Albacore (Thunnus alalunga). Aquat. Food Prod. Technol. 10 (3), 5–20. https://doi.org/10.1300/J030v10n03_02.

Sigfusson, H., Decker, E.A., McClements, D.J., 2001. Ultrasonic characterization of Atlantic mackerel (Scomber scombrus). Food Res. Int. 34 (1), 15–23. https://doi.org/10.1016/S0963-9969(00)00123-X.

Simmonds, J., MacLennan, D., 2005. Fisheries Acoustics, 2nd ed. Blackwell Science.

Spence, R.D., Granger, S., 2005. The scattering of sound from a prolate spheroid. J. Acoust. Soc. Am. 23 (6), 701. https://doi.org/10.1121/1.1906827.

Stanton, T.K., Chu, D., 2000. Review and recommendations for the modelling of acoustic scattering by fluid-like elongated zooplankton: euphausiids and copepods. ICES J. Mar. Sci. 57 (4), 793–807. https://doi.org/10.1006/jmsc.1999.0517.

Tang, Y., Nishimori, Y., Furusawa, M., 2009. The average three-dimensional target strength of fish by spheroid model for sonar surveys. ICES J. Mar. Sci. 66 (6), 1176–1183. https://doi.org/10.1093/icesjms/fsp080.

Wear, K.A., 2000. The effects of frequency-dependent attenuation and dispersion on sound speed measurements: applications in human trabecular bone. IEEE Trans. Ultrason. Ferroelectr. Freq. Control 47 (*1*), 265–273. https://doi.org/10.1109/58.818770.

Yasuma, H., Nakagawa, R., Yamakawa, T., Miyashita, K., Aoki, I., 2009. Density and sound-speed contrasts, and target strength of Japanese sandeel Ammodytes personatus. Fish. Sci. 75 (3), 545–552. https://doi.org/10.1007/s12562-009-0091-3.